PHYSICAL REVIEW D **80,** 122005 (2009)

Direct measurement of the anelasticity of a tungsten fiber

Shan-Qing Yang, Liang-Cheng Tu, Cheng-Gang Shao, Qing Li, Qing-Lan Wang, Ze-Bing Zhou, and Jun Luo*

Department of Physics, Huazhong University of Science and Technology, Wuhan 430074, People's Republic of China

(Received 7 September 2009; published 30 December 2009)

We report the first precision measurement of the frequency-dependent property of the effective torsion spring constant for a tungsten fiber by using two disk pendulums with different moments of inertia. A quartz fiber with $Q \approx 3.36 \times 10^5$ was used to determine the ratio of the moments of inertia of two pendulums. The experimental result indicated that the torsion spring constant of the tungsten fiber was dependent on the oscillation frequency by $\Delta K/\Delta(\omega^2) = (0.954 \pm 0.084) \times 10^{-8}$ kgm^2 at ~mHz range, which suggested that the resultant bias in our G measurement with the time-of-swing method was $\Delta G/G = (211.80 \pm 18.69)$ ppm as reported recently by Jun Luo *et al.* [Phys. Rev. Lett. **102**, 240801 (2009)]. This experiment provided the first direct test to the Kuroda-Newman effect that predicted an upward bias in a G measurement with the time-of-swing method.

DOI: 10.1103/PhysRevD.80.122005 PACS numbers: 04.80.Cc, 62.40.+i

I. INTRODUCTION

Precision measurements of the Newtonian gravitational constant G have widely been performed by using torsion balances with the time-of-swing (ToS) method [1–4], in which a pendulum suspended by a thin fiber would experience torsional oscillation in the gravitational field presented by source masses. With this method, torsional frequencies are compared for two different positions of the sources masses, and the difference of the frequencies squared $\Delta(\omega^2)$ is proportional to the Newtonian gravitational constant as $\Delta(\omega^2) = G/P_G$ with P_G being the gravitational coupling coefficient between the pendulum and the source masses.

The ToS method has a merit that it converts a small change of gravitational force into an obvious change of oscillation frequency, so that a high precision measurement can be achieved. The accuracy of the measurements of G with this method is severely dependent on the constancy of the spring constant of the fiber. However, the research works [5–10] on the frequency dependence of the fiber's spring constant suggested that a tremendous systematic error should occur in the measurements of G with the ToS method. This systematic upward bias induced by anelasticity of the fiber can be expressed in terms of G as

$$\frac{\Delta G}{G} = \frac{1}{I_G}\frac{K(\omega_n) - K(\omega_f)}{\omega_n^2 - \omega_f^2} = \frac{\Delta K}{I_G \Delta(\omega_{nf}^2)}, \tag{1}$$

where I_G is the moment of inertia (MoI) of the pendulum, ω_n and ω_f are the oscillation frequencies of the pendulum for the source masses at "near" and "far" positions, respectively.

The phenomenological model of an anelastic solid described by a single Maxwell unit (shown in Fig. 1) could be represented by a complex Young's modulus in the frequency domain as [11]

$$E(\omega) = \frac{\sigma(\omega)}{\epsilon(\omega)} = E_R + \delta E\left(\frac{\omega^2\tau^2}{1+\omega^2\tau^2} + \mathrm{i}\frac{\omega\tau}{1+\omega^2\tau^2}\right), \tag{2}$$

where E_R is the relaxed Young's modulus, δE is the difference between the unrelaxed and the relaxed modulus, and τ is the relaxation time. The real part of $E(\omega)$ corresponds to the real spring constant while its imaginary part represents the dissipation (or the phase lag). The behavior of the bulk elastic modulus of anelastic materials with a single relaxation process is well described by this simple Maxwell model over a certain frequency range [12,13]. However, in order to explain experimental results, a continuum Maxwell model (also shown in Fig. 1) was suggested by Quinn *et al.* [7], in which the Young's modulus can be expressed as

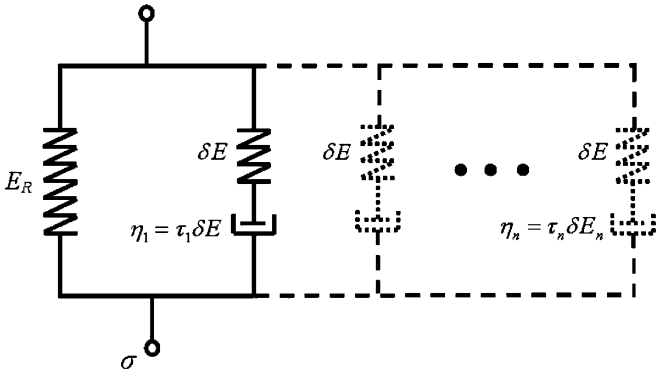

FIG. 1. The Maxwell model of an anelastic solid. The solid line shows the single Maxwell unit with an ideal spring shunted by a weaker spring in series with a dashpot. The total drawing shows the continuum Maxwell model suggested by Quinn *et al.* [7], which includes an infinite number of relaxation processes with a common relaxation strength δE but a continuum of time constants from a minimum τ_0 to a maximum τ_∞.

*junluo@mail.hust.edu.cn

$$E(\omega) = E_R + \frac{\delta E}{\ln(\tau_\infty/\tau_0)}\left[\frac{1}{2}\ln\left(\frac{1+\omega^2\tau_\infty^2}{1+\omega^2\tau_0^2}\right) + \mathrm{i}[\tan^{-1}(\omega\tau_\infty) - \tan^{-1}(\omega\tau_0)]\right], \quad (3)$$

where δE is the common relaxation strength, and τ_0 and τ_∞ represent the minimum and maximum time constant in a continuum spread of relaxation times, respectively. Quinn *et al.* [7] only evaluated the imaginary component of $E(\omega)$ in Eq. (3), and the frequency dependence of the real part was not discussed in detail.

The spring constant K of the fiber is proportional to the Young's modulus $E(\omega)$. It is not only a complex constant, but also frequency-dependent. Therefore, the torsion spring constant can be expressed as $K(\omega) = K_0 + K_1(\omega) + \mathrm{i}K_2(\omega) = K_r(\omega)[1 + \mathrm{i}\tan\phi(\omega)]$, where K_0 is the dominant component in the real part and frequency-independent, and $\phi(\omega)$ denotes losses (phase lag) in the weak spring. According to Eq. (1), the frequency-dependent real part is a well worth attention for the G measurement with the ToS method. Because of the unknown specific values for δE, τ_0 and τ_∞ in Eq. (3), Kuroda [5], further based on the Kramers-Kronig relation [14], supposed that the loss represented by the imaginary part is constant and concluded that the anelasticity of the fiber would lead an upward bias of $1/\pi Q$ in the measurements of G with the ToS method, where Q is the quality factor of the main torsional mode. Newman and Bantel [9] further demonstrated that, for the general continuum Maxwell model, the possible bias $\delta G/G$ due to the fiber's anelasticity should be bounded between 0 and $1/2Q$. The experimental evidence of this conjecture has been presented subsequently by Bagley and Luther [10] indirectly. In their G measurement, two fibers with different Q factors were used, and a wonderfully consistent value of G was obtained after corrected by $1/\pi Q$.

Up to now, most researchers paid more attention to the internal friction of materials in the field of gravitational physics [7,8], but few to the real part of the torsion spring constant directly. Kuroda and his colleagues [6] measured the frequency dependence of the real part of the torsion spring constant of a tungsten fiber directly, in which the MoI of the pendulum was changed by adjusting the positions of the masses on a dumbbell pendulum. Unfortunately, this experiment could not provide a definite result because of the geometrical errors of the pendulum. Furthermore, one crucial systematic error from the cross coupling between the local gravity gradient and the pendulum with different dumbbells, which resulted in a varied equivalent torsion constant in each measurement, was not discussed.

To reduce the anelasticity effect in G measurements with the ToS method, one possible approach is to use a fiber with an ultrahigh Q factor, like Newman's experiments performed in cryogenic condition [9]. Another operating approach in room temperature is to measure directly the frequency dependence of the real part of the torsion spring constant and then to deduct this effect correspondingly. In this paper we report a direct measurement of the anelasticity of a thoriated tungsten fiber, used in our G measurement [15], by using two disk pendulums with different MoIs and two fibers with different Q factors.

II. THE EXPERIMENTAL DESIGN

A. General principle

In order to determine the bias to the G value due to the anelasticity of the fiber, one can measure the MoIs I_1, I_2 and the corresponding eigen frequencies ω_1, ω_2 of two pendulums suspended by the same fiber alternately, and the anelastic effect of the fiber can be evaluated by

$$K_r(\omega_2) - K_r(\omega_1) = I_2\omega_2^2 - I_1\omega_1^2. \quad (4)$$

Considering the linearity of $K_r(\omega)$ in a limited frequency range [11], the correction due to the fiber's anelasticity, as shown in Eq. (1), could be further expressed as

$$\frac{\Delta G}{G} = \frac{I_2\omega_2^2 - I_1\omega_1^2}{I_G(\omega_2^2 - \omega_1^2)}. \quad (5)$$

Obviously, to measure G with an expected accuracy, the parameters ω_1, ω_2, I_1 and I_2 of two pendulums should be measured with the same relative accuracy correspondingly. However, it is more difficult to determine the MoIs than the oscillation frequencies of the pendulums, which was also a dominant error in the experiment of Kuroda and his colleagues [6]. In order to solve the problem, we rewrite Eq. (5) as

$$\frac{\Delta G}{G} = \frac{I_1}{I_G[(\omega_2/\omega_1)^2 - 1]}\left[\left(\frac{I_2}{I_1}\right)\left(\frac{\omega_2}{\omega_1}\right)^2 - 1\right]. \quad (6)$$

According to Eq. (6), we only need to determine the ratio I_2/I_1 (but not the I_1 or I_2 itself) with high accuracy, which could be realized by using a high-Q quartz fiber due to its negligible anelastic effect.

A schematic diagram of measuring the anelasticity of the tungsten fiber is shown in Fig. 2. Two fused silica disk pendulums with the same mass but different MoIs were suspended by a tungsten fiber and a quartz fiber alternately. The I_2/I_1 can be determined by measuring the free oscillation frequencies Ω_1, Ω_2 when two pendulums were suspended by the quartz fiber individually. Simply, we have $I_2/I_1 = \Omega_1^2/\Omega_2^2$. However, due to the different deviations among the centers of the disks and the fibers (as shown in Fig. 3), the MoIs of one pendulum suspended by the two fibers will be slightly different. The MoI of one pendulum system is composed of six components, expressed by

$$I = I_{\mathrm{disk}} + I_{\mathrm{clamp}} + I_{\mathrm{tube}} + I_{\mathrm{mirror}} + I_{\mathrm{glue}} + I_{\mathrm{coating}}, \quad (7)$$

where I_{disk}, the MoI of the disk, is a dominant component,

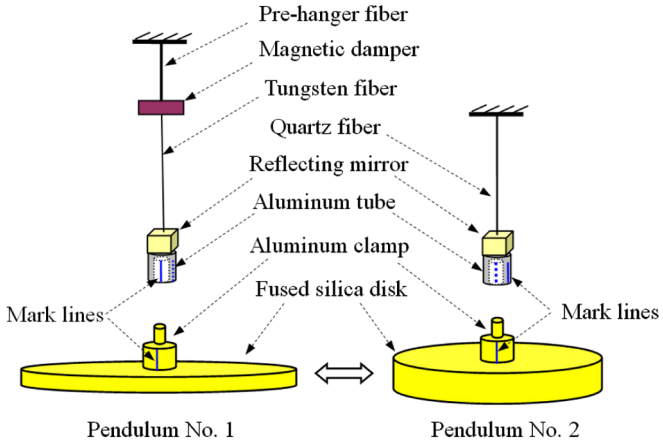

FIG. 2 (color online). Schematic drawing of two disk pendulums suspended by two fibers. A high-Q quartz fiber was used to determine the ratio of the moments of inertia I_2/I_1 by measuring the free oscillation frequencies Ω_1, Ω_2 of the two pendulums suspended by the quartz fiber alternately.

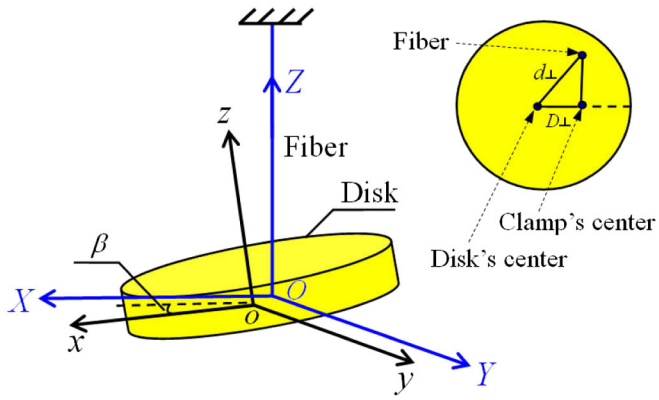

FIG. 3 (color online). The coordinate systems for calculating the moment of inertia of the fused silica disk. The coordinate system o-xyz is fixed on the disk with the origin at its geometric center o, and the other coordinate system O-XYZ is associated with the fiber, where the origin O is the mass center of the pendulum system, and β is the inclination angle of the disk. The inset shows the deviations ($d_\perp$ and $D_\perp$) among the centers of the disk, the clamp and the fiber, respectively.

and $I_{\rm clamp}$, $I_{\rm tube}$, $I_{\rm mirror}$, $I_{\rm glue}$ and $I_{\rm coating}$ are the MoIs of the clamp, the tube, the reflecting mirror, the glue used to adhere the fiber and the tube, and the gold-coated layer on the pendulum, respectively. For determining the $I_{\rm disk}$ conveniently, we define two coordinate systems as shown in Fig. 3. A Cartesian coordinate system o-xyz is fixed on the disk with the origin at its geometric center o, where the z-axis is the normal direction of the disk's plane, and the x-axis is along the inclined direction of the disk relative to the horizontal plane. The other coordinate system O-XYZ is associated with the fiber, where the origin O is the mass center of the pendulum system including the clamp, the tube and the mirror, etc., the Z-axis is along the fiber, and the Y-axis is parallel with the y-axis, which are both in the horizontal planes. The β represents the inclination angle of the disk. The detailed calculation shows that the MoI of the disk around the fiber can be expressed as

$$I_{\rm disk} = \frac{mr^2}{4}(1+\cos^2\beta) + \frac{mh^2}{12}\sin^2\beta + md_\perp^2, \quad (8)$$

where m, r and h are the mass, the radius and the height of the disk, respectively, and $d_\perp$, shown in Fig. 3, is the vertical distance from the center o to the fiber. Let $I_A = I_{\rm clamp} + I_{\rm tube} + I_{\rm mirror} + I_{\rm glue} + I_{\rm coating}$; the MoIs of two pendulums suspended by two fibers alternately can be calculated as

$$I_{ij} = \frac{m_j r_j^2}{4}(1+\cos^2\beta_{ij}) + \frac{m_j h_j^2}{12}\sin^2\beta_{ij} + m_j d_{\perp ij}^2 + I_{Aij}, \quad (i = W, Q, j = 1, 2.), \quad (9)$$

where the subscripts "W" and "Q" represent the tungsten fiber and the quartz fiber, respectively, and "1" and "2" denote the pendulums No. 1 and No. 2, respectively. According to Eq. (9), the ratio I_2/I_1 can be expressed as

$$\frac{I_2}{I_1} = \frac{I_{W2}}{I_{W1}} \simeq \frac{I_{Q2}}{I_{Q1}}(1+\varepsilon), \quad (10)$$

where $I_{Q2}/I_{Q1} = \Omega_1^2/\Omega_2^2$, and the parameter ε, accounting for the tiny differences of the MoIs, is calculated as

$$\varepsilon = \frac{\frac{m_1 r_1^2}{4}(\cos^2\beta_{Q1} - \cos^2\beta_{W1}) + \frac{m_1 h_1^2}{12}(\sin^2\beta_{Q1} - \sin^2\beta_{W1}) + m_1(d_{\perp Q1}^2 - d_{\perp W1}^2) + (I_{AQ1} - I_{AW1})}{I_{Q1}} - \frac{\frac{m_2 r_2^2}{4}(\cos^2\beta_{Q2} - \cos^2\beta_{W2}) + \frac{m_2 h_2^2}{12}(\sin^2\beta_{Q2} - \sin^2\beta_{W2}) + m_2(d_{\perp Q2}^2 - d_{\perp W2}^2) + (I_{AQ2} - I_{AW2})}{I_{Q2}}. \quad (11)$$

One logical question would be naturally presented after the above discussion: Why do we not use the high-Q quartz fiber instead of the tungsten fiber to perform the G measurement with the ToS method? The reason is that the lack of conductivity of the uncoated quartz fiber prevented an accurate determination of the oscillation period of the torsion pendulum, while the metallic coating on a quartz fiber would spoil the Q sharply and hence mitigate most of the advantages of this material [16]. In our G measurement, the pendulum must be designed as a dipole to sensitize the

gravitational effect of the source masses, thus it is also sensitive to electrostatic effect. While in this experiment, the pendulums were designed to be symmetric disks with a thin gold-coated layer on the surface and surrounded by a thin hollow gold-coated aluminum shielding cylinder, keeping a wider separation between the pendulum and the shielding cylinder than that in our G measurement, the influence of local electrostatic field was minimized evidently.

B. Apparatus

Two similar vacuum chambers were used to perform this measurement. In one chamber, an annealed and thoriated tungsten fiber (Th0.6/W99.4) [17] with a length of 89 cm and a diameter of 25 μm was used. A schematic apparatus is shown in Fig. 4. The pendulum was suspended by the fiber, and the upper end of the fiber was attached to a magnetic damper to suppress the simple pendulum motions [18]. The copper disk of the damper was suspended by a 10-cm-long, 50-μm-diameter annealed tungsten prehanger fiber, which was finally linked to a feedthrough fastened on the top of the vacuum chamber. The feedthrough was used to adjust the initial amplitude and the azimuth of the torsion pendulum.

In another chamber, a quartz fiber without the magnetic damper was used to determine the ratio I_2/I_1. In order to obtain a higher-Q factor, the diameter of the quartz fiber should be much thicker due to diameter-dependent dissipation [19]. After several tests, a quartz fiber with a length of 48 cm and a diameter of about 100 μm was finally chosen to perform this experiment. The average quality factor of this fiber was $Q \approx 3.36 \times 10^5$ in repeated experiments.

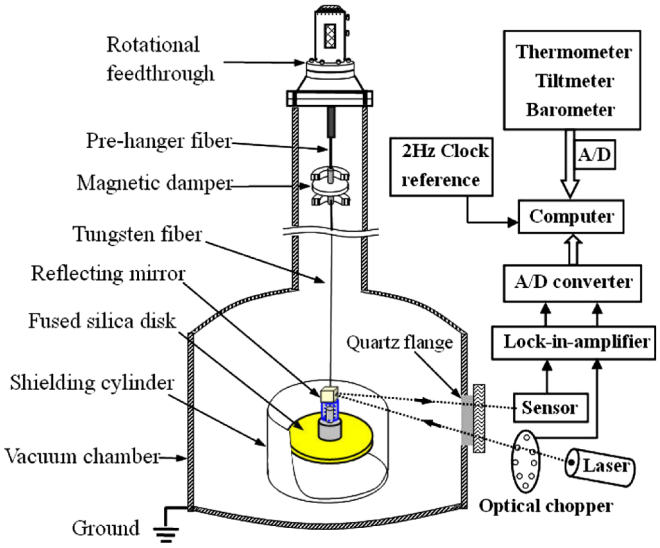

FIG. 4 (color online). Schematic view of the apparatus used to measure the anelasticity of a tungsten fiber, where the ion pump was not shown.

The vacuum chambers were maintained at a pressure of $\sim 10^{-5}$ Pa by ion pumps [20]. The whole apparatus was surrounded by the foam houses, which provided the effective thermal insulation. The experiment site was located in our cave laboratory.

The oscillation of the pendulum was monitored by an optical lever. A laser beam from a frequency-stabilized He-Ne laser ($\Delta\nu/\nu \leq 1 \times 10^{-8}$/day, $P = 0.6$ mW) passed through an optical chopper [21], and then was reflected by a mirror attached on the fiber. The reflected beam of light fell on a position sensor [22], which was placed about 500 mm far from the mirror. The differential signal from the position sensor went through a lock-in-amplifier [23] and then was converted into a series of time-angle data by a 16-bit A/D converter [24], and was finally sampled at a rate of 2 Hz with a frequency accuracy of $\pm 5 \times 10^{-9}$ Hz and a stability of $\leq 3 \times 10^{-10}$/day [25]. Two thermal sensors installed inside each chamber monitored the temperature variations continuously. The free oscillation periods of the two pendulums, suspended by the tungsten fiber, respectively, were about 581.2 s and 488.2 s, and covered the range of the periods in our G measurement [15]. The periods of the two pendulums suspended by the quartz fiber were about 29.6 s and 35.3 s, correspondingly.

C. Pendulums

Each pendulum system includes four parts: the fused silica disk, the clamp, the tube and the reflecting mirror, as shown in Fig. 2. The main bodies of the pendulums are two gold-coated fused silica disks with masses of 63.6545(6) and 63.6937(6) g, diameters of 68.725(4) and 81.794(7) mm, and heights of 7.8031(2) and 5.5148(1) mm, respectively. The aluminum clamp, adhered to the center of

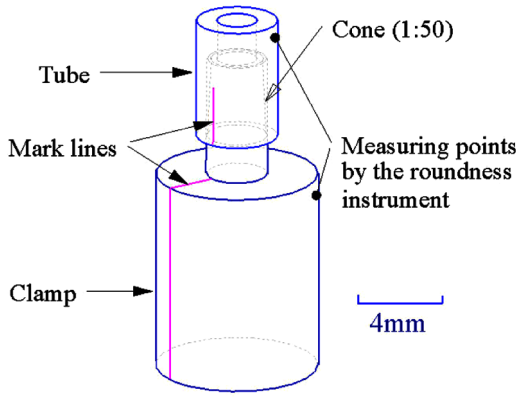

FIG. 5 (color online). Schematic view of measuring the eccentricities between the clamps and the tubes by a roundness measuring instrument. By rotating the tube around the clamp, an appropriate azimuth with minimum eccentricity was found, and then two lines were marked on the tube and the clamp, respectively, which were aligned elaborately in each experiment to lower the difference of the moments of inertia of one pendulum suspended by different fibers alternately.

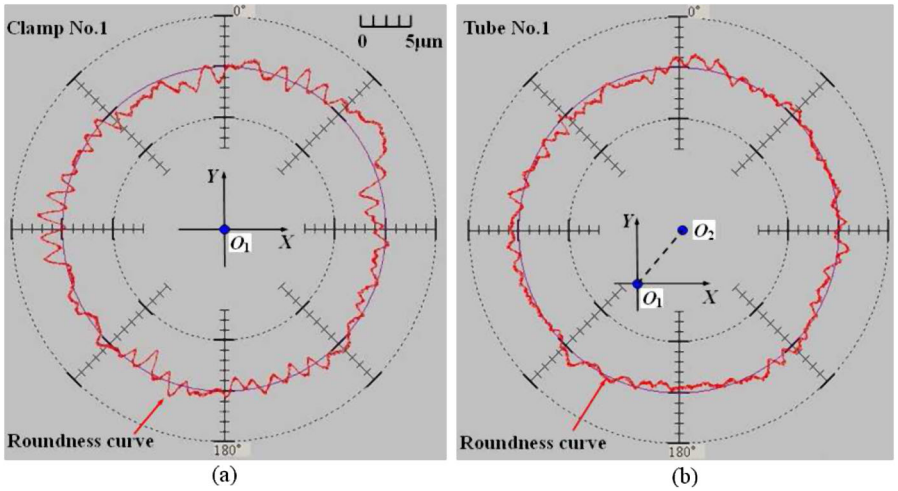

FIG. 6 (color online). Typical curves for measuring the roundness and the eccentricities of the clamps and the tubes. (a): The typical result of the clamp No. 1 with a roundness of 5.88(40) μm, and the center O_1 was regarded as the reference. (b): The typical result of the tube No. 1 with a roundness of 3.43(18) μm, and the average eccentricity is $O_1O_2 = 17.40(1.56)$ μm obtained by several repeated measurements.

the disk pendulum with uncertainties of 3 μm by using an optics image measuring instrument [26], was connected to the aluminum tube by inserting the 1:50 cone cylinder into the same 1:50 conical hole in the tube, as shown in Fig. 5. The aluminum tube was adhered centrically to the fiber with an uncertainty within 13 μm. On the top of the aluminum tube, a gold-coated cubical glass with a cylindric hole was adhered to act as the reflecting mirror.

The eccentricities of different combinations between the two clamps and the two tubes were measured alternately under a roundness measuring instrument [27] with an accuracy within 0.03 μm. The schematic diagram is also shown in Fig. 5. First, the center and the roundness of one cylindrical clamp were measured, and the center O_1 was regarded as a reference point, as shown in the top panel in Fig. 6. Then, one of the tubes was fitted onto the clamp, and its center and roundness were measured again. By rotating the tube around the clamp, an appropriate azimuth with minimum eccentricity was found, and then two lines were marked on the tube and the clamp, respectively, (as shown in Fig. 5). Finally, the repeatability of assembly was measured and found to be within an error of less than 2 μm by aligning the mark lines on the clamps and the tubes. The measured results of alternately assembling the clamps and the tubes are listed in Table I.

The inclination of the two pendulums suspended by the two fibers were measured by a micrometer, as shown in Fig. 7. First, the lowest point of the pendulum's bottom plane was measured by adjusting the micrometer to touch the bottom slightly, and the scale of the micrometer h_1 was recorded. Then the pendulum was twisted by 180 ° around the fiber, and the topmost point of the bottom plane was measured by heightening the micrometer, and the scale was h_2. So the inclination angle of the pendulum was calculated by $\beta = \sin^{-1}[(h_2 - h_1)/D]$, where D is the diameter of the disk. After four sets of measurements, the inclination angles were obtained to be $\beta_{W1} = 3.06(6)$ mrad, $\beta_{W2} = 4.61(10)$ mrad (when the two pendulums were suspended by the tungsten fiber alternately) and $\beta_{Q1} = 3.79(8)$ mrad, $\beta_{Q2} = 4.05(12)$ mrad (suspended by the quartz fiber alternately). Finally, according to Eq. (11), the parameter ε was determined as

TABLE I. The eccentricities of different combinations between two clamps and two tubes. (unit: μm).

Number	Clamp No. 1	Clamp No. 2
Tube No. 1	17.40(1.56)	17.07(1.22)
Tube No. 2	13.14(0.62)	23.41(0.70)

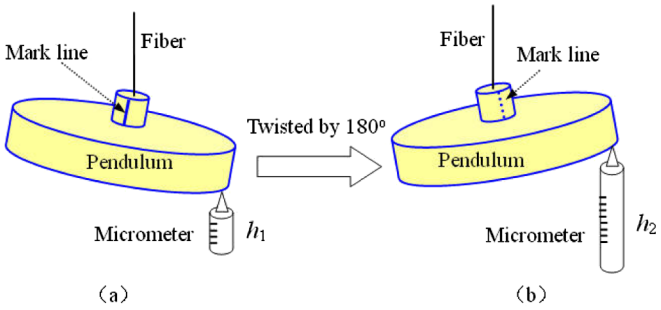

FIG. 7 (color online). Schematic view of measuring the inclination angle of one pendulum suspended by one fiber. A micrometer was used to measure the height difference Δh between the lowest point (a) and the topmost one (b) of the disk's bottom plane, then the inclination angle of the pendulum relative to the horizontal plane was $\beta = \sin^{-1}(\Delta h/D)$ with D being the diameter of the disk.

TABLE II. The one σ error budget of the parameter ε.

Source	Value (error)	$\Delta\varepsilon(\times 10^{-6})$
Disk No. 1		0.36
mass m_1	63.6937(6) g	
diameter $2r_1$	81.794(7) mm	
height h_1	5.5148(1) mm	
inclination angle β_{W1}	3.06(6) mrad	
inclination angle β_{Q1}	3.79(8) mrad	
center departure $d_{\perp W1}$	0.5(7) μm	
center departure $d_{\perp Q1}$	0.5(7) μm	
Disk No.2		0.66
mass m_2	63.6545(6) g	
diameter $2r_2$	68.725(4) mm	
height h_2	7.8031(2) mm	
inclination angle β_{W2}	4.61(10) mrad	
inclination angle β_{Q2}	4.05(12) mrad	
center departure $d_{\perp W2}$	0.8(6) μm	
center departure $d_{\perp Q2}$	0.8(7) μm	
Other moments of inertia (kgm^2)		0.48
I_{AW1}	$5.2077(45)\times 10^{-8}$	
I_{AW2}	$3.4332(44)\times 10^{-8}$	
I_{AQ1}	$5.1996(45)\times 10^{-8}$	
I_{AQ2}	$3.4248(45)\times 10^{-8}$	
Total	-4.14×10^{-6}	0.89

$$\varepsilon = (-4.14 \pm 0.89)\times 10^{-6}. \quad (12)$$

The one σ error budget for the parameter ε is shown in Table II.

III. SYSTEMATIC ERRORS

A. Gravity gradient and its compensation

Because the disk pendulum was not spherical symmetric and its inclination was not zero, the inhomogeneous background gravitational field would contribute a gravitational torsion constant $K_g(\theta)$ to the pendulum system, and it can be expressed as

$$K_g(\theta) = \frac{\partial^2 V_g(\theta)}{\partial\theta^2}, \quad (13)$$

where $V_g(\theta)$ is the gravitational potential energy between the pendulum and the background gravitational field, and θ is the azimuth of the pendulum. Therefore, the pendulum's oscillation frequency squared becomes

$$\omega^2(\theta) = \frac{K_r + K_g(\theta)}{I}, \quad (14)$$

where I is the MoI of the pendulum, and K_r is the torsion spring constant of the fiber. The existence of the $K_g(\theta)$, depending on mass distribution of the pendulum and the surrounding masses, would introduce a systematic error in the measurement of the pendulum's frequency.

In order to measure this effect easily, we deliberately exaggerated it by using a gold-coated glass rectangular pendulum with dimensions of $91\times 26\times 12$ mm^3 (shown in Fig. 8), which is more sensitive to the local gravity gradient than the disk one, to measure the change of period when the equilibrium position of the pendulum was shifted to different azimuths. We changed the pendulum's azimuth with a step of 30 degrees every time by rotating the feedthrough, and then the corresponding oscillation period of the pendulum was measured with an optical lever, in which a twelvefold-mirror, linked on the pendulum's center, was used to reflect the laser beam. The experiment

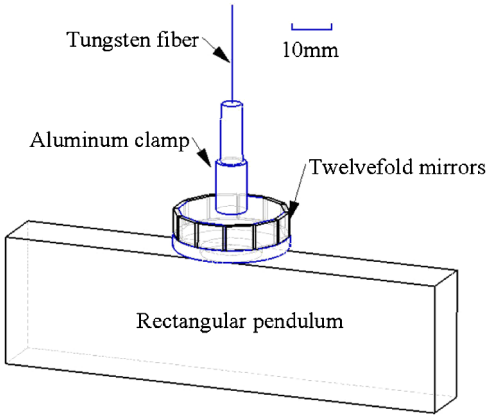

FIG. 8 (color online). The rectangular pendulum used to measure the cross coupling effect between the background gravity gradient and the pendulum. The twelvefold symmetric mirrors linked on the pendulum's center are used to reflect the laser beam of monitoring the oscillation motion of the pendulum when at each different azimuth.

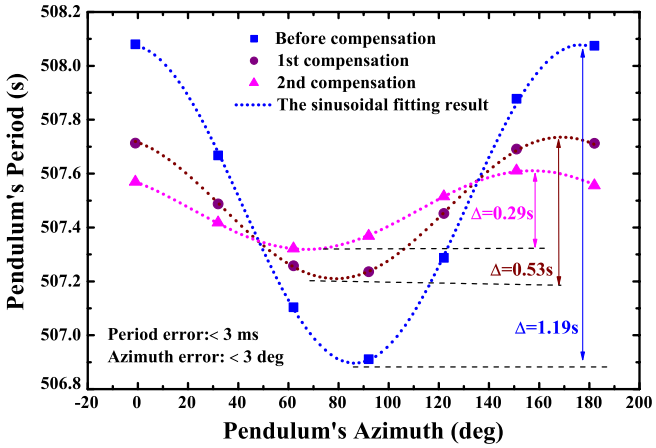

FIG. 9 (color online). The measured period shifts due to the cross coupling between the local gravity gradient and the rectangular pendulum. Each point represents the average period of about 60 consecutive oscillations of the pendulum at a certain azimuth. The dot lines represent the sinusoidal fitting results, which show that the maximum shift of the period was about 1.19 s with the pendulum's azimuth changed from 0 to 180°, then it was minimized to about 0.29 s after ~1.5 tons of lead blocks compensation.

result showed that the maximum shift of the period was about 1.19 s when the pendulum's azimuth was changed from 0 to 180°. Then the lead blocks of ~1.5 tons were used to compensate the local inhomogeneous gravitational field. After careful adjustment, the final period's shift of the rectangular pendulum was within 0.29 s, as shown in Fig. 9. It means that the homogeneity of the local gravity is improved about 4 folds. In this case, we can estimate that the maximum shift of the oscillation period of the disk pendulum was about 0.01 ms if the equilibrium position of the pendulum changed in a range of 10 mrad at any azimuth with the maximum inclination angle of $\beta_{W2} = 4.61(10)$ mrad measured. Considering the angle linear drift of the fiber (~ 3 μrad/h), it will take about 140 days to change the pendulum's azimuth to 10 mrad, which is enough for us to carry out our experiment without considering the gravity gradient effect.

B. Thermoelastic property of the torsion fiber

The torsion spring constant of an ideal torsion fiber can be expressed as

$$K = \frac{\pi r^4 S}{2l}, \tag{15}$$

where l and r are the fiber's length and radius, respectively, $S = E/2(1 + \mu)$ is the shear modulus and E and μ are the Young's modulus and Poisson's ratio of the fiber, respectively. Because the parameter l, r and E are the linear functions of temperature in a limited range [11], the spring constant of the fiber is temperature-dependent, named as the thermoelastic. For a small temperature change $\Delta t(= t - t_0)$, the torsion spring constant can be expressed by [11]

$$K = K_0(1 + \alpha_K \Delta t), \tag{16}$$

where α_K is the temperature coefficient of K, and K_0 is the torsion spring constant at the reference temperature t_0. The α_K can be determined by measuring the temperature coefficient of the pendulum period α_T, defined as

$$\alpha_T = \frac{\Delta T}{T \Delta t}, \tag{17}$$

where ΔT is the change of the period with the variation of temperature Δt. The pendulum's period is $T = 2\pi\sqrt{I/K}$, so α_K is relative to α_T as

$$\alpha_K = \alpha_I - 2\alpha_T, \tag{18}$$

where α_I is the temperature coefficient of the MoI of the pendulum. Therefore, we can measure the changes of the pendulum's period with the variation of the room temperature and then determine α_T and α_K, correspondingly.

We investigated the thermoelastic property of the two fibers (used in the measurement of anelasticity) by means of the method described in Ref. [28]. Six 60 W bulbs, concealed by six metal barrels, were placed in the outside of the foam house as the heating sources to modulate the room temperature. Two thermal sensors with resolution of 0.0005 °C were placed in the chamber near the fiber and the pendulum, respectively. The oscillation signals of the pendulum were monitored by an optical lever synchronically. The periods were extracted from the angle-time data by a correlative method [29]. The typical changes of the pendulum's period and the ambient temperature were shown in Fig. 10. After three sets of experiments, we obtained two coefficients: $\alpha_{KW} = -145(2) \times 10^{-6}/°C$ for the tungsten fiber and $\alpha_{KQ} = 131(2) \times 10^{-6}/°C$ for the quartz fiber, respectively. It is noted that the torsion spring constant of the tungsten fiber K_W represented a commonly negative dependence on temperature as discussed in Refs. [11,12]. Contrarily, the K_Q of the quartz fiber took on a positive temperature-dependence, which is

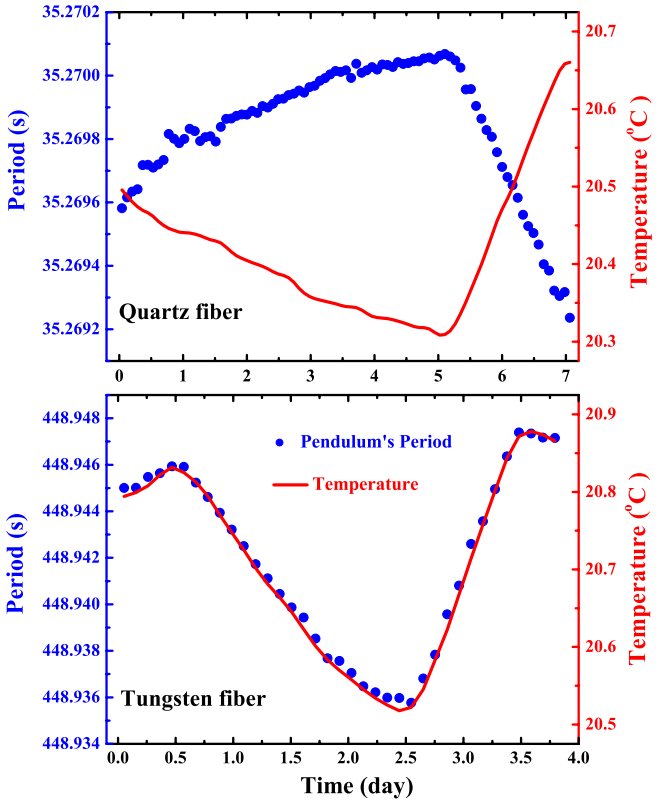

FIG. 10 (color online). Typical curves of the pendulums' period and the ambient temperature varied with time for the two fibers. Top panel: the quartz fiber suspended with the pendulum No. 1. Bottom panel: the tungsten fiber with the pendulum No. 2. Each circle point represents the average period of 200 oscillations for the quartz fiber and 15 ones for the tungsten one. The solid lines show the change of the modulated ambient temperature correspondingly, which was changed about 0.35 °C in this measurement.

relative to the configuration and intension of the Si-O bonds in quartz materials and it is consistent with previous experimental results [30].

C. Nonlinearity property of the torsion fiber

If we consider the nonlinear property of the fiber, the typical equation of the oscillation of the pendulum should be written as

$$I\ddot{\theta} + K_1\theta + K_3\theta^3 = 0, \tag{19}$$

where I and θ are the MoI and the angle displacement of the pendulum, respectively, and the coefficient K_3 represents the nonlinearity of the fiber. The approximate solution of Eq. (19) at a small amplitude oscillation can be expressed as [9,31]

$$\theta(t) \approx A\cos\omega t + \frac{K_3}{32K_1}A^3\cos 3\omega t, \tag{20}$$

where A is the amplitude of the oscillation, and the period $T(=2\pi/\omega)$ of the pendulum would vary with its amplitude A as

$$T(A) \approx T_0\left(1 - \frac{3}{8}\kappa_3 A^2\right), \tag{21}$$

where $T_0 = 2\pi\sqrt{I/K_1}$ is the unperturbed period of the pendulum, and $\kappa_3 = K_3/K_1$ is the nonlinearity coefficient of the fiber. The fiber's amplitude dependence of oscillation frequency was measured in the following procedure. For the tungsten fiber, the pendulum was started to oscillate with an initial amplitude of ~11 mrad, and it gradually attenuated to ~2.5 mrad due to the fiber's dissipation in four days, and then the feedthrough was adjusted to reset the pendulum to almost the same initial amplitude for the next set of the experiment. For the quartz fiber, due to its high-Q factor, its amplitude was attenuated by adjusting the feedthrough directly.

The typical pendulum's period and amplitude varied with time and are shown in Fig. 11. The result showed that the change of the period with time was not due to the nonlinearity of the fiber, because the corresponding jump of the period did not occur when the amplitude was reset. Obviously, a time-dependent effect of the period was included, which was the so-called aging effect of the fiber as observed in our G measurement [15]. Therefore, due to different aging effects of two fibers, we used the goal functions of

$$T_W(A) = T_{W0}\left(1 - \frac{3}{8}\kappa_{W3}A^2\right) + \delta T_{W0}(1 - e^{-b_W t}) + \gamma_W t \tag{22}$$

and

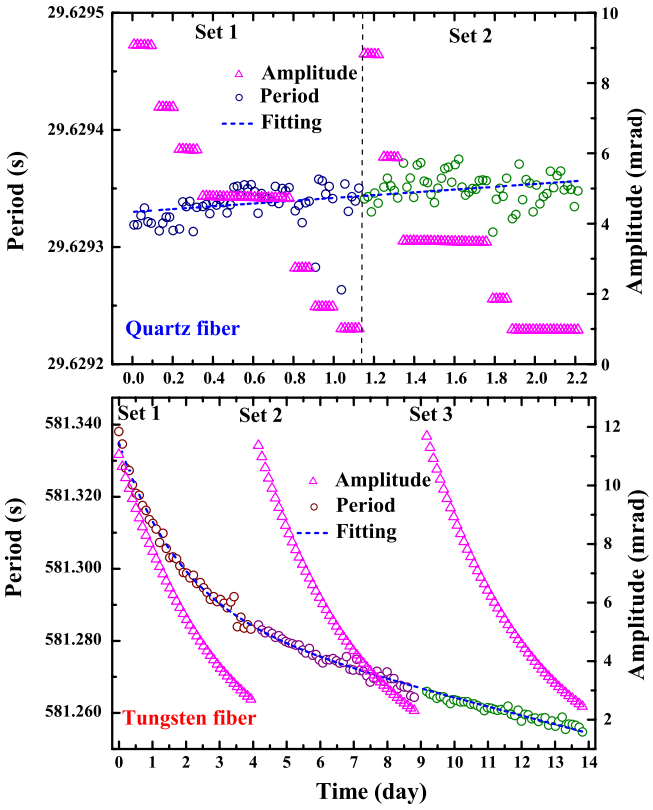

FIG. 11 (color online). Pendulums' period and amplitude varied with time for the two fibers. Top panel: the quartz fiber suspended with the pendulum No. 2. Bottom panel: the tungsten fiber with the pendulum No. 1. Each circle represents the average period of 50 oscillations for the quartz fiber and 15 ones for the tungsten fiber, and each triangle shows the change of oscillation amplitude correspondingly. The pendulum was reset to the same initial amplitude in the next set of the experiment to distinguish the nonlinearity and the aging effect of the fiber. The dashed lines represent the fitting results as Eqs. (22) and (23), respectively, which showed that the period was independent of the amplitude of the pendulum.

$$T_Q(A) = T_{Q0}\left(1 - \frac{3}{8}\kappa_{Q3}A^2\right) + \gamma_Q t \tag{23}$$

to fit the periods, amplitudes and times with the nonlinear least-squares method for the two fibers, respectively. In Eqs. (22) and (23), the parameters κ_{W3} and κ_{Q3} are nonlinearity coefficients of the tungsten fiber and the quartz one, respectively. The γ_W and γ_Q represent the linear aging effect of the two fibers, respectively, and the b_W denotes

TABLE III. Measurement results of the nonlinearity of the two fibers.

Fiber	κ_3(/rad^2)	γ(ms/day)	b_W(ms/day)
Tungsten fiber	0.005(12)	−1.77(6)	0.52(2)
Quartz fiber	0.004(7)	0.011(3)	···

the exponential aging effect of the tungsten fiber due to the slow recovery after being reloaded at the beginning of each set of experiment. The fitting results are listed in Table III, and show a null effect for the nonlinearity, but an opposite linear aging effect for the two fibers due to the hardening and softening behavior for the tungsten fiber and the quartz one, respectively.

IV. EXPERIMENTAL RESULTS

A. Data accumulation

At the beginning of each measurement, the initial amplitudes of the pendulums were adjusted to be the same as possible. Twelve sets of experimental data with two pendulums suspended by the quartz fiber (four sets) and the tungsten fiber (eight sets) alternately were taken. It took about five days for each measurement of one pendulum suspended by one fiber in our previous ten sets of experiments. According to the result obtained from this data, the periods of the pendulum suspended by the quartz fiber showed a much better stability than that by the tungsten one. Therefore, only four sets of experimental data for the quartz fiber were enough to achieve the precision required.

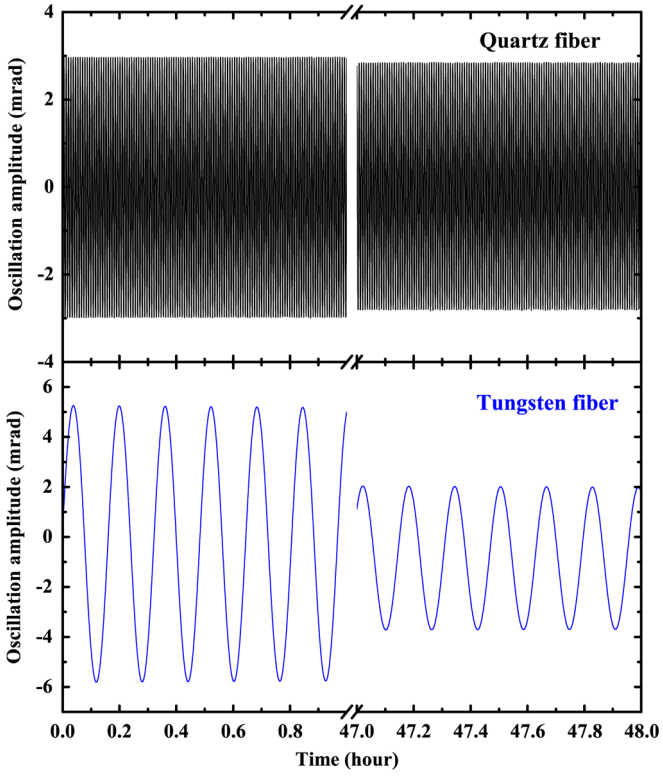

FIG. 12 (color online). One typical cut of the pendulum's angle-time data of 48 hours. Top panel: oscillations of the pendulum No. 2 suspended by the quartz fiber. Bottom panel: oscillations of the pendulum No. 1 suspended by the tungsten fiber. The average Q factors of the quartz fiber was $\sim 3.36 \times 10^5$ while the tungsten fiber was ~ 1700 yielded from all experimental data.

In order to reduce the uncertainty of the pendulum's period when suspended by the tungsten fiber, eight sets of experiments were repeated. It is noted that the duration of last two sets of experiments was extended to 15 days, and the motivation was to deduct the exponential aging effect at the beginning of each reloading the tungsten fiber, also shown in the bottom panel in Fig. 11.

B. Data analysis protocol

The typical oscillation of the pendulums is shown in Fig. 12. The quality factor is defined as the logarithmic decrement in terms of the amplitudes A_{n+1} and A_n of the $(n+1)$th and nth oscillations of the pendulum as

$$Q^{-1} = \frac{1}{\pi} \ln\left(\frac{A_n}{A_{n+1}}\right). \tag{24}$$

For the oscillation with the quartz fiber, the amplitude decayed from 2.97(1) mrad to 2.81(1) mrad with a duration of 48 h, which corresponded to 5833 periods with a single period of $T_0 = 29.6$ s for the pendulum No. 2, thus the quality factor was obtained to be 3.31×10^5 according to Eq. (24). The average Q factors of $\sim 3.36 \times 10^5$ (for the quartz fiber) and ~ 1700 (for the tungsten fiber) were obtained from all experimental data.

A typical variation of the temperature with a 15-day duration is shown in Fig. 13. At the beginning of each experiment, the temperature raised to $\sim 22\,^\circ$C due to the working of the turbopump, and then it decreased to a

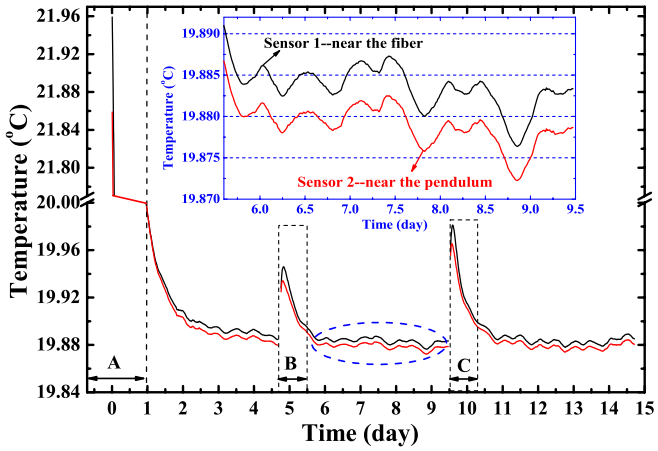

FIG. 13 (color online). The typical variation of the ambient temperature with a 15-day duration. The region "A" denoted a rapid decreasing process of the temperature from $\sim 22\,^\circ$C (raised due to the working of the turbopump at the beginning of each experiment) to the experimental temperature $\sim 20\,^\circ$C by putting several barrels of ice blocks in the room within 24 hours. The regions "B" and "C" represented a slightly larger variation of the temperature induced by people going in the room to reset the pendulum by adjusting the feedthrough every five days. The inset shows the detailed variation of the temperature of two thermal sensors ranged from 5.6 to 9.5 d, and the average temperature of two sensors was used in the data analysis.

normal temperature ~20 °C by putting several barrels of ice blocks in the room within 24 hours. In each set of measurement, the variation of the temperature was less than 0.1 °C in 5-day experimental duration. The total variation of the temperature was about 0.3 °C over the entire duration of the experiments. The periods were all corrected to 20.0 °C by means of the temperature coefficients α_{KW} and α_{KQ} measured, which contributed an error of <0.2 ms for the tungsten fiber and <0.01 ms for the quartz one, respectively.

The periods of 12 data sets are shown in Fig. 14. In order to obtain the ratio of the frequencies squared in Eqs. (6) and (10), the "A-B-A" method was used to deduce the linear aging effect of each fiber. After being corrected by the effect of the magnetic damper as described in Ref. [15], the average ratio of the frequencies squared of two pendulums suspended by the tungsten fiber was yielded as

$$\left(\frac{\omega_2}{\omega_1}\right)^2 = 1.4171723(92). \tag{25}$$

And the ratio of the frequencies squared of the quartz fiber was

$$\left(\frac{\Omega_1}{\Omega_2}\right)^2 = 0.7056861(5). \tag{26}$$

According to Eqs. (10) and (12), the ratio I_2/I_1 of two pendulums suspended by the tungsten fiber was obtained as

$$\frac{I_2}{I_1} = 0.7056832(8). \tag{27}$$

According to Eq. (6), we can obtain that the torsion spring constant was dependent on the pendulum's oscillation frequency squared as

$$\frac{\Delta K}{\Delta(\omega^2)} = (0.954 \pm 0.084) \times 10^{-8}\ \text{kgm}^2, \tag{28}$$

with $I_1 = 5.3318(8) \times 10^{-5}$ kgm^2 obtained by measuring the geometry dimensions and the mass of the pendulum No. 1. It means that, taking $I_G = 4.505679(35) \times 10^{-5}$ kgm^2 into account [15], the correction to G due to the anelasticity of the thoriated tungsten fiber was

$$\frac{\Delta G}{G} = (211.80 \pm 18.69)\ \text{ppm}, \tag{29}$$

which was the largest uncertainty attributed to our G measurement [15], and the one σ error budget of the anelasticity to $\Delta G/G$ is shown in Table IV.

From Table IV, the main uncertainty was due to the stability of the periods of the pendulums suspended by the tungsten fiber. It was mainly caused by the frequent reloading of the tungsten fiber when exchanging the pendulums every 5 or 15 days, which resulted in a larger exponential aging effect at the beginning of each data set and thus affected the period's repeatability. To improve the stability of the periods, a possible approach is to further

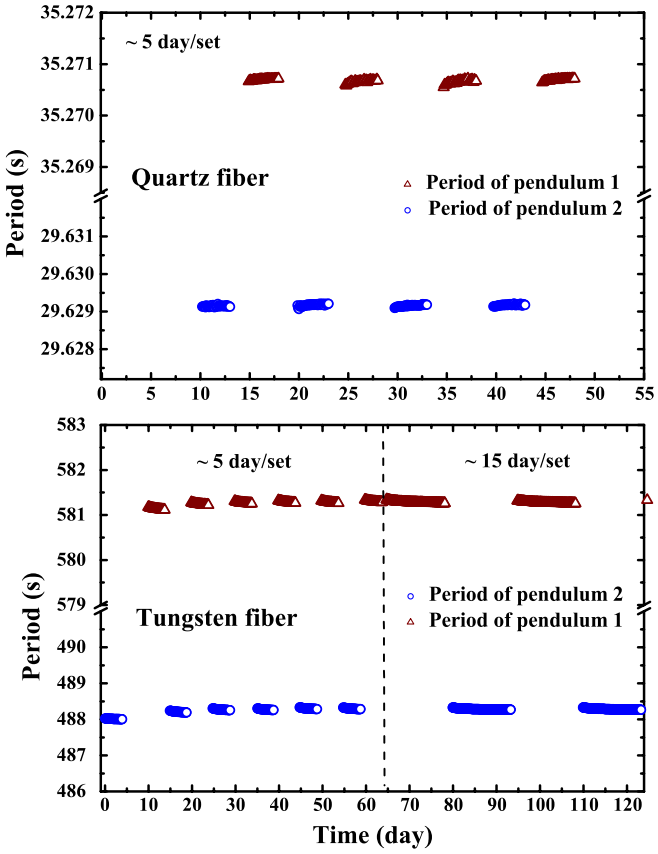

FIG. 14 (color online). The oscillation periods of the pendulums suspended by the quartz fiber and the tungsten one alternately, which were extracted from the angle-time data by a correlative method and were corrected by the thermoelastic property (α_{KW} and α_{KQ}) of the fibers. Top panel: the periods for the quartz fiber with a duration of 5 days for each measurement, where each point represents the average period of 200 oscillations. Bottom panel: the periods for the tungsten fiber with a duration of 5 days for the previous six sets of data and 15 days for the last two sets, where each point represents the average period of 15 oscillations.

TABLE IV. One σ uncertainty budget of the anelasticity to $\Delta G/G$.

Source	Value (error)	ppm	
I_1	$5.3318(8) \times 10^{-5}$ kgm^2		0.03
I_G	$4.505679(35) \times 10^{-5}$ kgm^2		0.00
Magnetic damper		4.78	
Statistical $(\omega_2/\omega_1)^2$	1.4171723(92)		18.41
Statistical $(\Omega_1/\Omega_2)^2$	0.7056861(5)	2.01	
ε	$-4.14(89) \times 10^{-6}$	2.52	
$\frac{I_2}{I_1} = (\frac{\Omega_1}{\Omega_2})^2(1+\varepsilon)$	0.7056832(8)		3.22
Total			18.69

extend the duration of each measurement when the pendulum is suspended by the tungsten fiber.

V. CONCLUSIONS

In summary, we have directly measured the anelastic effect of the thoriated tungsten fiber used in our G measurement with the ToS method. The experimental result indicates that the torsion spring constant of the tungsten fiber is frequency-dependent at ~mHz range. With the fiber's quality factor Q of the main torsional mode being about 1700, the measured quantity of the correction to the G value seems to be slightly larger than the limit of $1/\pi Q$ predicted by Kuroda [5], but smaller than the upper bound of $1/2Q$ predicted by Newman [9]. This measurement suggests that the anelasticity of the fiber is still one of the major sources of the systematic uncertainties in the G measurement with the ToS method.

However, the distinct advantages of the ToS method are so attractive that it will be chosen in our future G measurement. The anelastic behavior of different fibers, such as the pure tungsten fiber and the Be-Cu one, will be explored by means of the method described in this paper, by which some common characteristics could be found and the fiber's anelasticity could be understood sufficiently.

In addition, a high-Q quartz fiber will be used in our future G measurement. To reduce the electrostatic effect due to the lack of conductivity of the uncoated quartz fiber, a charge-management (or ultraviolet illumination discharging) technique could be utilized such as in GP-B [32] and LISA [33]. Furthermore, recent research work about the coating loss on the fiber's surface suggested that it was possible to make a conductive quartz fiber with a lower mechanical loss. A quality factor of $Q \sim 1.6 \times 10^5$ of a fused silica fiber had been obtained after coated by a thin germanium (Ge) and bismuth (Bi) layer [34], which provided an important indication for improving the sensitivity of the torsion pendulum in our next experiment.

ACKNOWLEDGMENTS

We are very appreciative of Riley Newman for detailed discussions on the design of this experiment. We also wish to thank Kazuaki Kuroda and Zhong-Zhu Liu for their helpful discussions. This work is supported in part by the National Basic Research Program of China under Grant No. 2010CB832801, the National High-Tech Research and Development Plan of China under Grant No. 2008AA12A215, and the National Natural Science Foundation of China under Grant No. 10805021.

[1] P. R. Heyl, J. Res. Natl. Bur. Stand. **5**, 1243 (1930).
[2] G. G. Luther and W. R. Towler, Phys. Rev. Lett. **48**, 121 (1982).
[3] O. V. Karagioz, V. P. Izmaylov, and G. T. Gillies, Gravitation Cosmol. **4**, 239 (1998).
[4] J. Luo, Z. K. Hu, X. H. Fu, S. H. Fan, and M. X. Tang, Phys. Rev. D **59**, 042001 (1998).
[5] K. Kuroda, Phys. Rev. Lett. **75**, 2796 (1995).
[6] S. Matsumura, N. Kanda, T. Tomaru, H. Ishizuka, and K. Kuroda, Phys. Lett. A **244**, 4 (1998); K. Kuroda, Meas. Sci. Technol. **10**, 435 (1999).
[7] T. J. Quinn, C. C. Speake, and L. M. Brown, Philos. Mag. A **65**, 261 (1992); C. C. Speake, T. J. Quinn, R. S. Davis, and S. J. Richman, Meas. Sci. Technol. **10**, 430 (1999).
[8] P. R. Saulson, R. T. Stebbins, F. D. Dumont, and S. E. Mock, Rev. Sci. Instrum. **65**, 182 (1994); P. R. Saulson, Phys. Rev. D **42**, 2437 (1990).
[9] R. D. Newman and M. K. Bantel, Meas. Sci. Technol. **10**, 445 (1999); M. K. Bantel and R. D. Newman, J. Alloys Compd. **310**, 233 (2000).
[10] C. H. Bagley and G. G. Luther, Phys. Rev. Lett. **78**, 3047 (1997).
[11] C. Zener, *Elasticity and Anelasticity of Metals* (University of Chicago Press, Chicago, 1948).
[12] T. S. Kê, Phys. Rev. **71**, 533 (1947); J. Alloys Compd. **211–212**, 7 (1994).
[13] A. S. Nowick and B. S. Berry, *Anelastic Relaxation in Crystalline Solids* (Academic, New York, 1972).
[14] H. A. Kramers, Nature (London) **117**, 775 (1926); R. de L. Kronig, J. Opt. Soc. Am. **12**, 547 (1926).
[15] J. Luo, Q. Liu, L. C. Tu, C. G. Shao, L. X. Liu, S. Q. Yang, Q. Li, and Y. T. Zhang, Phys. Rev. Lett. **102**, 240801 (2009).
[16] E. G. Adelberger, J. H. Gundlach, B. R. Heckel, S. Hoedl, and S. Schlamminger, Prog. Part. Nucl. Phys. **62**, 102 (2009); C. Hagedorn, S. Schlamminger, and J. H. Gundlach, AIP Conf. Proc. **873**, 189 (2006).
[17] Goodfellow Cambridge Limited, Huntingdon PE29 6WR, England.
[18] Y. Tu, L. Zhao, Q. Liu, H. L. Ye, and J. Luo, Phys. Lett. A **331**, 354 (2004); X. D. Fan, Q. Liu, L. X. Liu, V. Milyukov, and J. Luo, Phys. Lett. A **372**, 547 (2008).
[19] A. M. Gretarsson and G. M. Harry, Rev. Sci. Instrum. **70**, 4081 (1999); S. D. Penn, G. M. Harry, A. M. Gretarsson, S. E. Kittelberger, P. R. Saulson, J. J. Schiller, J. R. Smith, and S. O. Swords, Rev. Sci. Instrum. **72**, 3670 (2001).
[20] SP-400, Shanghai Shanjin Vacuum Equipment Co. Ltd, Shanghai, China.
[21] SR540, Stanford Research Systems Company, USA.
[22] SL1352, Hamamatsu Photonics K. K, Japan.
[23] SR830, Stanford Research Systems Company, USA.
[24] PCI-6014, National Instruments Company, USA.
[25] EE1620C, Nanjing Telecommunication Instruments Factory, Nanjing, China.
[26] JVT-250, Guiyang Xintian Oetech Co. Ltd, Guizhou, China.

[27] DTP-1000B, Guangzhou Wilson Precision Instruments Co. Ltd, Guangzhou, China.
[28] J. Luo, Z. K. Hu, and H. Hsu, Rev. Sci. Instrum. **71**, 1524 (2000).
[29] F. Chen, S. C. Wu, S. H. Fan, and J. Luo, Meas. Sci. Technol. **14**, 619 (2003); Y. L. Tian, Y. Tu, and C. G. Shao, Rev. Sci. Instrum. **75**, 1971 (2004).
[30] H. D. H. Drane, Proc. R. Soc. A **122**, 274 (1929); J. V. Atanasoff and P. J. Hart, Phys. Rev. **59**, 85 (1941).
[31] Z. K. Hu, J. Luo, and H. Hsu, Phys. Lett. A **264**, 112 (1999).
[32] S. Buchman, T. Quinn, G. M. Keiser, and D. Gill, Rev. Sci. Instrum. **66**, 120 (1995).
[33] T. Sumner, H. Araújo, D. Davidge, A. Howard, C. Lee, G. Rochester, D. Shaul, and P. Wass, Classical Quantum Gravity **21**, S597 (2004).
[34] K. Numata, J. Horowitz, and J. Camp, Phys. Lett. A **370**, 91 (2007).